



Cite this: DOI: 10.1039/c8dt03007c

Exploring (bio)catalytic activities of structurally characterised Cu(II) and Mn(III) complexes: histidine recognition and photocatalytic application of Cu(II) complex and derived CuO nano-cubes†

Babli Kumari,^a Samapti Kundu,^b Kajari Ghosh,^a Mahuya Banerjee,^a Swapan Kumar Pradhan,^b Sk. Manirul Islam,^c Paula Brandão,^d Vitor Félix^d and Debasis Das^a

Structurally characterised two polymeric complexes of Cu(II) (**3**) and Mn(III) (**4**) of the ligand L (2-(((2-(phenylamino)ethyl)imino)methyl)phenol) have been explored for catecholase-like activity, fluorescence recognition of histidine and catalytic activity towards coupling of aryl iodides with benzamide, leading to *N*-arylbzamidates. CuO nano-cubes (NCs) prepared by thermal decomposition of the Cu(II) complex function as photocatalysts for the degradation of methylene blue. Cube-like morphology of CuO nano-crystal and flake-shaped micrometer order Cu(II) complex have been established from the field emissive scanning electron microscopy (FESEM) images.

Received 23rd July 2018,
Accepted 2nd September 2018

DOI: 10.1039/c8dt03007c

rsc.li/dalton

Introduction

Schiff's base-derived copper and manganese complexes are used as multi-functional materials.^{1–7} Recently, copper complexes of Schiff's bases have found potential applications as sensors and in catalytic, anti-viral and anti-bacterial activities. They may deactivate HIV or H1N1 virus also.⁸

On the other hand, manganese is an essential trace metal for the development and functioning of the brain.⁹ It acts as a cofactor for several enzymes such as decarboxylase, hydrolase and kinase that are involved in the metabolism of protein, lipid and carbohydrate.¹⁰ Unusual concentration of manganese in brain, especially in basal ganglia, results in neurological disorders identical to Parkinson's disease.¹¹ In human and animal tissues, the concentration of manganese is less than 1 $\mu\text{g g}^{-1}$ wet weight,¹² whereas its function is poorly understood.

These facts inspired us to report polymeric complexes of copper and manganese of a Schiff base derivative and study their activities such as molecular sensing, catecholase activity and catalytic activity.

It is well-known that histidine (His) is an essential amino acid for human growth, particularly for children's growth and repair of human tissues.¹³ His plays a vital role in several proteins through metal–ligand coordination or acid–base catalysis with the imidazole moiety collectively with carbonic anhydrase.¹⁴

The unusual level of His-rich protein causes several diseases in humans.¹⁵ The impaired nutritional state of patients with chronic kidney disease may be ascribed to the deficiency of His.¹⁶ It is reported as a neurotransmitter or neuromodulator in the mammalian central nervous system.¹⁷ It is pertinent to mention that the biological importance of His has opened up an active research area for the development of optical probes in recent years.¹⁸ Therefore, several methods for the determination of His have been suggested, *viz.*, liquid chromatography,^{19,20} capillary electrophoresis,^{21,22} voltammetry,²³ spectrofluorimetry^{24–30} and spectrophotometry.^{31,32} However, recognition of His by fluorescence spectroscopy is demanding due to its operational simplicity, rapidity, non-invasiveness and less expensive methodology, direct and instant visual perception, selectivity and sensitivity.^{33,34} Several metal complexes have been used as fluorescence and colorimetric probes for His.^{35,36} In the light of previous studies, we have prepared a Cu(II) complex that acts as a turn on, highly selective probe for His over other amino acids.

^aDepartment of Chemistry, The University of Burdwan, Burdwan, 713104 W.B., India. E-mail: ddas100in@yahoo.com

^bDepartment of Physics, The University of Burdwan, Burdwan, 713104 W.B., India

^cDepartment of Chemistry, University of Kalyani, Kalyani, Nadia, 741235, India

^dDepartment of Chemistry, CICECO – Aveiro Institute of Materials, University of Aveiro, 3810-193 Aveiro, Portugal

†Electronic supplementary information (ESI) available: Contains NMR, FTIR, UV-Vis, fluorescence spectra. CCDC 1052606 (**3**) and 1827168 (**4**). For ESI and crystallographic data in CIF or other electronic format see DOI: 10.1039/c8dt03007c

Catechol oxidase catalyses oxidation of a wide range of *o*-diphenols (catechols) to corresponding *o*-quinones.^{37–44} This catecholase activity depends on several factors such as metal–metal distance, structure of ligands, its electrochemical properties, and pH of the medium. Literature suggests that some Mn(III),⁴⁵ Mn(IV)⁴⁶ and a few Mn(II) complexes⁴⁷ exhibit catecholase-like activity, whereas phenol-based ligands have rarely been used. Mohanta *et al.*⁴⁸ have reported a series of Mn(III) complexes that show catecholase activity with turnover (K_{cat}) numbers in between 17.0–41.7 h⁻¹ in DMF and 16.9–137.3 h⁻¹ in MeCN. Several mononuclear^{49–51} and dinuclear^{52–55} Cu(II) complexes show significant catecholase-like activities. However, catecholase activity of polymeric metal complexes is relatively rare.

On the other hand, the most proficient and potent method for the synthesis of *N*-aryl amide is transition metal-catalyzed cross coupling reaction between aryl halide and amide, and it has immense importance in biological, pharmaceutical and material research.⁵⁶

It is well-known that amidation of aryl halides has efficiently been achieved by using palladium catalyst.⁵⁷ However, copper-catalysed amidation is rare.⁵⁸ The low cost, environmentally friendly nature and easy availability allow copper to be an attractive catalyst for C–N cross-coupling reactions.

Surface and ground water contamination by organic pollutants released from textile industries is a serious concern and highly alarming for human and wild life. Photo-catalysis has emerged as a promising green technique for the degradation of organic pollutants in wastewater.⁵⁹ Copper oxide, a *p*-type semiconductor having a narrow band gap (1.2–2.5 eV), acts as an excellent photo-catalyst for the degradation of organic pollutants.⁶⁰ Thermal decomposition of copper complex is an inexpensive, well-known and relatively new method for the preparation of highly pure CuO nanostructures, which prompted us to prepare CuO nanostructures from our new Cu(II) complex.^{61,62}

Overall, we report the synthesis of two polymeric complexes of Cu(II) and Mn(III) using a reported Schiff's base.⁶³ The structures of the complexes are confirmed by single crystal X-ray diffraction analysis. The catecholase-like activities of the complexes have been demonstrated. The Cu(II) complex selectively recognizes His by fluorescence spectroscopy, supported by other techniques. Moreover, the Cu(II) complex acts as an efficient catalyst for coupling several aryl iodides with benzamide to yield the respective *N*-arylbenzamides. Additionally, CuO nano-cubes (NCs) prepared by thermal decomposition of the Cu(II) complex function as an efficient photo-catalyst for visible light-driven decomposition of a representative organic contaminant: methylene blue (MB) dye.

Results and discussion

Single crystal X-ray structures of Cu(II) complex (3) and Mn(III) complex (4)

Single crystals of 3 and 4 suitable for X-ray diffraction were grown from methanol–dichloromethane mixture (1:1, v/v). The most relevant structural features of 3 and 4 are depicted in

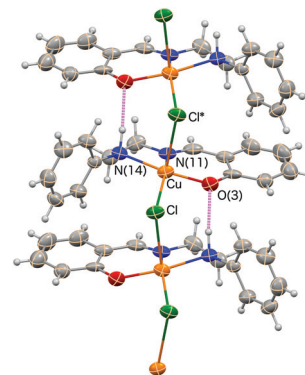


Fig. 1 A single polymeric chain $[\text{CuL}_2\text{Cl}]_n$ of 3 in crystalline state. Thermal ellipsoid drawn at the 50% probability level and the N–H...O hydrogen bonds are drawn as violet dashed lines. *Symmetry operator: $x, 1/2 - y, 1/2 + z$.

Fig. 1 and 2 including thermal ellipsoids and $[\text{ML}_2\text{Cl}]_n$ polymeric chains formed in solid state. Selected bond lengths and angles around metal centres are summarized in Table 1.

In 3, Cu(II) centres are covalently linked by chloride with non-equivalent Cu–Cl distances of 2.286(2) and 2.849(3) Å and an angle Cu–(μ -Cl)–Cu of 105.22(8)°, leading to the formation of one dimensional polymeric chain with a ladder shape (Fig. 1). Furthermore, the phenolate and amine groups of the adjacent ligands (L) interact through almost linear hydrogen bonds (N...O = 2.967(9) Å and $\angle\text{N–H...O} = 170.0^\circ$). This structure has a distorted square-pyramidal geometry with a structural index of trigonality $\tau = (\beta - \alpha)/60^\circ = 0.32$, where α and β are the *trans*-angles N(11)–Cu–Cl and N(1)–Cu–Cl of 172.2(2) and 152.8(2)°, respectively.⁶⁴ The basal plane is composed of nitrogen and phenol oxygen donors from the tridentate L and bridging chloride with shorter Cu–Cl distance. The apical position is occupied by the remaining bridging chloride at much longer Cu–Cl distance (*ca.* 0.6 Å difference) than that expected for a d^9 Cu(II) complex due to Jahn–Teller distortion.

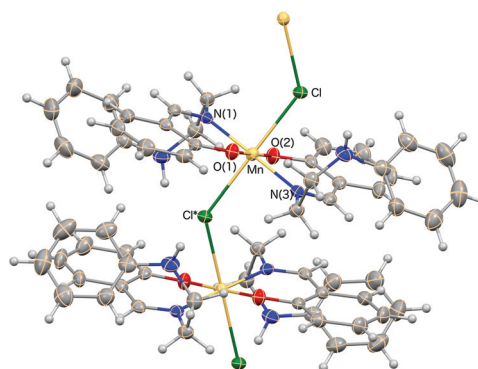


Fig. 2 A single $[\text{MnL}_2\text{Cl}]_n$ polymeric chain of 4 in crystalline state. *Symmetry operator: $-1/2 + x, y, 3/2 - z$. Remaining details are given in Fig. 1.

Table 1 Selected bond lengths (Å) and angles (°) in **3** and **4**

Complex 3			
Cu–Cl	2.286(2)	Cu–Cl ^(b)	2.849(3)
Cu–O(3)	1.912(6)	Cu–N(14)	2.060(7)
Cu–N(11)	1.967(6)		
Cl–Cu–Cl ^(b)	107.64(8)	Cu–Cl–Cu ^(a)	105.22(8)
O(3)–Cu–N(11)	91.8(3)	O(3)–Cu–Cl	90.32(16)
O(3)–Cu–N(14)	172.2(2)	N(11)–Cu–Cl	152.75(19)
Cl–Cu–N(14)	97.44(18)	Cl ^(b) –Cu–O(3)	94.86(17)
N(11)–Cu–N(14)	81.7(3)	Cl ^(b) –Cu–N(11)	99.26(18)
Cl ^(b) –Cu–N(14)	82.01(19)		
Complex 4			
Mn–Cl	2.6127(10)	Mn–Cl ^(a)	2.6080(10)
Mn–O(31)	1.864(2)	Mn–N(39)	2.032(3)
Mn–N(19)	2.034(3)	Mn–O(11)	1.869(2)
Mn–Cl–Mn ^(b)	130.39(3)	N(39)–Mn–N(19)	179.08(11)
Cl–Mn–Cl ^(a)	179.25(4)	O(31)–Mn–O(11)	178.93(11)
O(31)–Mn–N(39)	90.33(10)	O(11)–Mn–N(19)	90.71(10)

For complex **3**, (a) and (b) stand for symmetry operators $x, 1/2 - y, -1/2 + z$ and $x, 1/2 - y, 1/2 + z$, respectively. For complex **4**, (a) and (b) denote the symmetry operators $-1/2 + x, y, 3/2 - z$ and $1/2 + x, y, 3/2 - z$, respectively.

In **4**, Mn(III) centres are also covalently assembled in polymeric zigzag chains (Fig. 2) by chloride bridges with slightly different Mn–Cl distances of 2.608(1) and 2.613(1) Å and an obtuse Mn–Cl–Mn angle of 130.39(3)°. Moreover, each Mn(III) centre exhibits an octahedral environment with the chloride bridges occupying the axial positions ($\angle\text{Cl–Mn–Cl} = 179.25(4)^\circ$), whereas the four equatorial sites are occupied by nitrogen and oxygen donors from 2-(iminomethyl) phenol moieties of two independent L ligands. In other words, in contrast to that observed for the Cu(II) complex, both L ligands adopt bidentate behaviour and therefore, their amino nitrogen centres are away from the manganese centre. The Mn–O distance of 1.864(2) Å and Mn–N distances of 2.035(3) and 2.032(3) Å are similar to those observed in the manganese polymeric complex of 2-ethoxy-6-[[[2-(phenylamino)ethyl] imino] methyl] phenolato (Mn–N, 2.044(2) and Mn–O, 1.862(1) Å), in which octahedral Mn(III) centres are also linked by chloride bridges with Mn–Cl distances of 2.617(1) Å.⁶⁵

Interactions with amino acids (AA)

The fluorescence response of **L** (5 μM) towards Cu²⁺ was tested in HEPES (20 mM, 0.1 M, ethanol/water, 1/1, v/v, pH 7.4) (Fig. S1, ESI[†]). Upon gradual addition of Cu²⁺, the emission intensity of **L** at 440 nm gradually decreases and gets finally quenched. The fact that Cu²⁺ complex selectively distinguishes His from other AAs⁶⁶ made us test **3** as a potential candidate for fluorescence recognition of His. The emission intensity of **3** enhances eleven-fold upon interaction with His ($\lambda_{\text{em}} = 440$ nm, $\lambda_{\text{ex}} = 380$ nm) (Fig. 3), whereas other natural AAs (Trp, Cys, Phe, Gly, Thr, Ile, Pro, His, Arg, Ger, Met, Lys, Leu, Glu, Gla, Asp, Asn, Gln, Val, Tyr) do not exhibit any interference (Fig. 4). However, **4** does not show any fluorescence enhancement upon interaction with these AAs. Emission intensities of **3** have been examined in the presence and absence of His at different pH values (Fig. S2, ESI[†]). However, the physiological

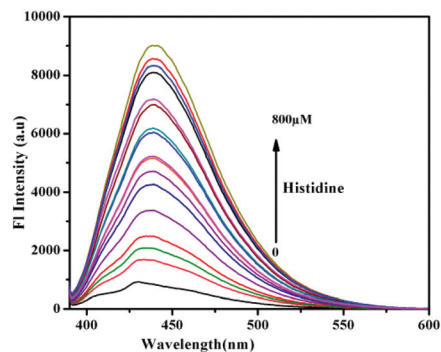


Fig. 3 Changes in fluorescence spectra of **3** (5 μM) in HEPES buffer (0.1 M, ethanol/water, 1/1, v/v, pH 7.4) upon gradual addition of His (800 μM) ($\lambda_{\text{ex}} = 380$ nm; $\lambda_{\text{em}} = 440$ nm).

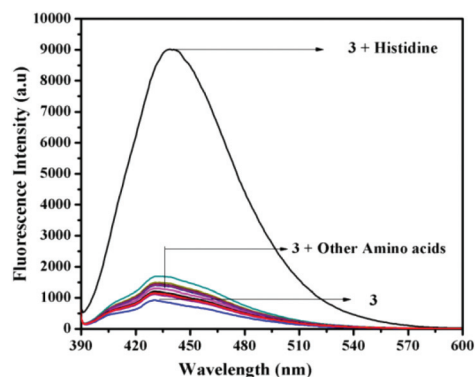


Fig. 4 Relative emission intensities of **3** upon addition of different AAs (100 μM) in said medium, $\lambda_{\text{ex}} = 380$ nm.

pH of 7.4 has been selected for entire studies. No significant interference from other AAs is observed (Fig. S3, ESI[†]). The lowest detection limit and binding constant for His are 5.66×10^{-8} M and 4.34×10^4 M⁻¹, respectively (Fig. S4 and 5, ESI[†]). The plot of emission intensity of **3** vs. [His] is shown in Fig. S6 (ESI[†]), the linear region of which is useful for the determination of an unknown concentration of His. The fluorescence quantum yield of **3** increases from 0.24 to 0.72 in the presence of His.

His extracts out Cu(II) from **3** and releases free ligand. Hence, emission intensity that is enhanced at 440 nm is due to free ligand.⁶⁷

The ESI-MS spectrum of the mixture of His and **3** provides a molecular ion peak at 371.17 (Fig. S7, ESI[†]), indicating the formation of [2His + Cu²⁺] adduct. An intense peak at 241.53 indicates the release of free ligand. Job's plot also indicates the same stoichiometry (Fig. S8, ESI[†]). The probable sensing mechanism is illustrated in Scheme 2.

Catecholase-like activity

Catecholase-like activities of **3** and **4** have been studied using 3,5-di-tertiarybutyl catechol (DTBC) for its low redox potential and easy monitoring of absorbance at ~400 nm (corres-

Table 2 Kinetic parameters of catecholase-like activity of **3** and **4**

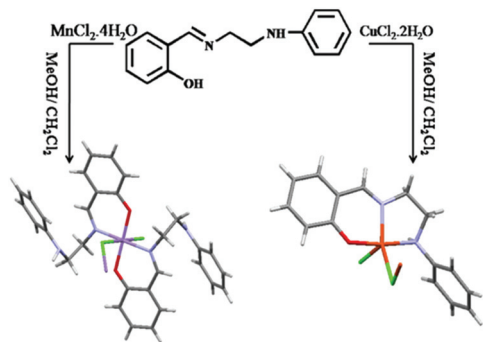
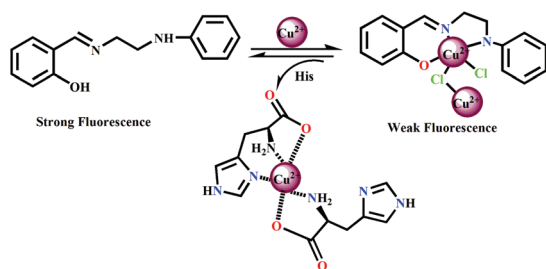
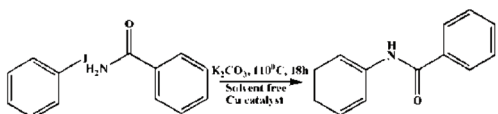
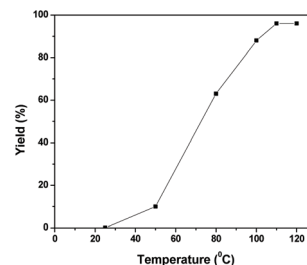
Complex	V_{\max} (M s^{-1})	K_M (M)	k_{cat} (h^{-1})
3	2.72×10^{-4}	6.36×10^{-3}	9.79×10^3
4	2.79×10^{-4}	1.13×10^{-3}	1.00×10^4

ponding *o*-quinone, DTBQ). The rate constant (turn over number, K_{cat}), maximum velocity (V_{\max}) and binding constant (K_M) are calculated from the plot of $1/V$ vs. $1/[S]$ (Fig. S9 to S16, ESI† and Table 2) using the equation $1/V = \{KM/V_{\max}\} \times \{1/[S]\} + 1/V_{\max}$.

Catalytic activity

The catalytic activities of **3** towards *N*-arylation of amide have been tested by reacting iodobenzene and benzamide under solvent-free conditions (Scheme 1).

As bases play a key role in the efficiency of the *N*-amidation reaction between aryl iodide and benzamide, the reactions are monitored by varying moderate to strong bases. It is observed that the yield is highest with K_2CO_3 , which is a mild base (Table S2, ESI,† entry 5) (Scheme 3).

**Scheme 1** Synthesis of **3** and **4**.**Scheme 2** Probable sensing mechanism.**Scheme 3** A model *N*-arylation reaction using **3** as catalyst.**Fig. 5** Optimization of reaction temperature (iodobenzene, 1.0 mmol; benzamide, 1.2 mmol; K_2CO_3 , 1.3 mmol; catalyst, 10 mg; time, 18 h; solvent free). The yield is monitored with GC.

On the other hand, solvent also plays a crucial role towards product yield. Hence, both polar and non-polar solvents have been screened. However, no significant improvement has been observed (Table S3, ESI,† entries 1–3). Hence, the reaction is screened under solvent-free conditions and interestingly, better efficiency is observed (Table S3,† entry 4). The catalytic reaction does not occur at room temperature. While gradual increase of temperature increases the yield, the optimum temperature has been observed as 110 °C (Fig. 5) (Table 3).

Nanostructure characterization of CuO nano-cubes (CuO NCs)

Fig. 6 shows the Rietveld analysis of PXRD of CuONCs derived by calcination of **3**. The peak positions match well with the

Table 3 *N* arylation reaction with Cu catalyst

Entry	R	Product	Yield (%)
1	H		96
2	4-OMe		89
3	4-Me		92
4	2-Me		89
5	2-NH ₂		88
6	4-NO ₂		97
7	4-Cl		78

Reaction conditions: Iodobenzene (1.0 mmol), benzamide (1.2 mmol), K_2CO_3 (1.3 mmol), solvent (2.5 mL), catalyst (10 mg), 18 h, 110 °C. GC yield.

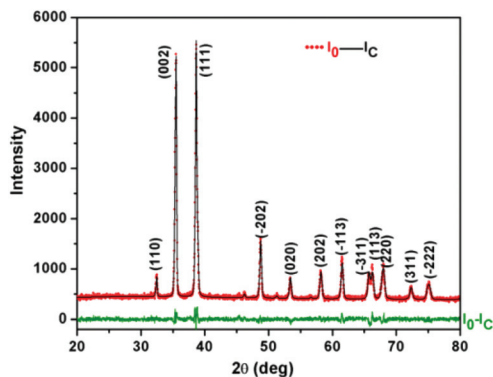


Fig. 6 Observed (red) PXRD patterns and corresponding Rietveld powder structure refinement output patterns (black) of CuONCs. ($I_o - I_c$) is the difference between observed and calculated patterns.

monoclinic polycrystalline CuO phase (JCPDF No. 41-0254; space group, $C2/c$, monoclinic; a , 4.685 Å; b , 3.423 Å; c , 5.132 Å and β , 99.52°). All peaks are indexed accordingly. The well-resolved sharp peaks indicate crystallite (coherently diffracting domain) CuO, which is almost free from lattice strain. The most interesting part in this pattern is the intensity of the (002) reflection, which is almost the same as the strongest reflection of CuO powder. The ideal $I_{002} : I_{111}$ for CuO powder is 0.6 (JCPDF No. 41-0254), which becomes 0.95 for Cu NCs, indicating orientation of cubes along the (002) plane. The results confirm preferential growth of NCs along $\langle 002 \rangle$, which is obtained by incorporating the March–Dollase function in the Rietveld refinement.⁶⁸ The refined structural and micro-structural parameters are presented in Table S4 (ESI†).

Determination of surface morphology by FESEM

Field emission scanning electron microscopy (FESEM) has been employed to determine the morphology and size of micro-flakes of **3** and CuO NCs derived from it. Fig. 7a reveals that **3** consists of different micro-flakes agglomerated together

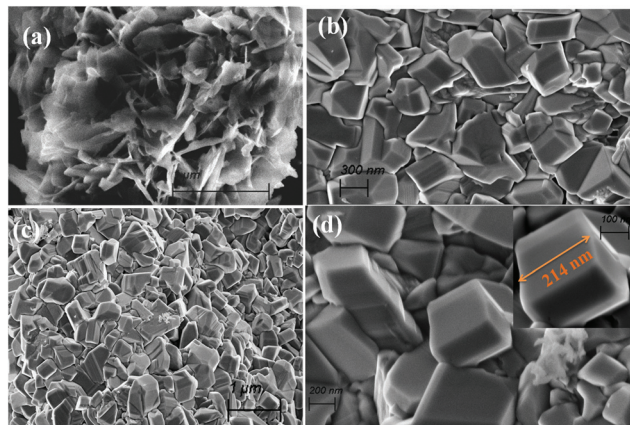


Fig. 7 FESEM images of (a) Cu(II) complex, (b–d) CuO NCs at low and high magnifications.

to form a bundle. Cube-like CuO nano-crystals have been produced uniformly after calcination of **3** (Fig. 7b–d). A single distinct cube shown in the inset of Fig. 7d has side length of ~214 nm, which is well corroborated with the Rietveld refinement value (Table S4, ESI†). PXRD analysis of the residue obtained after calcination of **3** indicates CuO. Thus, a morphological evolution from continuous 2D micro-flakes to 3D cube-like CuO NCs with preferential growth along $\langle 002 \rangle$ has been observed.

Photo-catalytic activity of CuONCs under visible light

The photo-catalytic activity of CuO NCs for the degradation of methylene blue (MB), an organic pollutant dye, has been explored. The absorbance of MB decreases gradually with increasing time upon visible light illumination (Fig. 8a). In the presence of CuO NCs, the absorbance of MB reduces to ~20% within 4 h. The reaction follows pseudo first order kinetics $\ln(C_0/C) = kt$, where C_0 and C are concentrations of MB before and after visible light illumination, respectively. The first order rate constant (k) has been found to be $6.84 \times 10^{-3} \text{ min}^{-1}$ (Fig. 8b). The mechanism of photo-degradation of MB is portrayed in Scheme 4. The visible solar radiation has much higher energy than the band gap of CuO photo-catalyst (~2.62 eV).

Absorption of photons with energies equal to or exceeding the band gap of CuO NCs generates electron–hole pairs. For MB degradation, photo-induced holes in the VB readily react with the hydroxyl ions (hole acceptors) to form hydroxyl radicals ($\cdot\text{OH}$) with the generation of corresponding photo-excited electrons at CB, which react with dissolved O_2 to generate

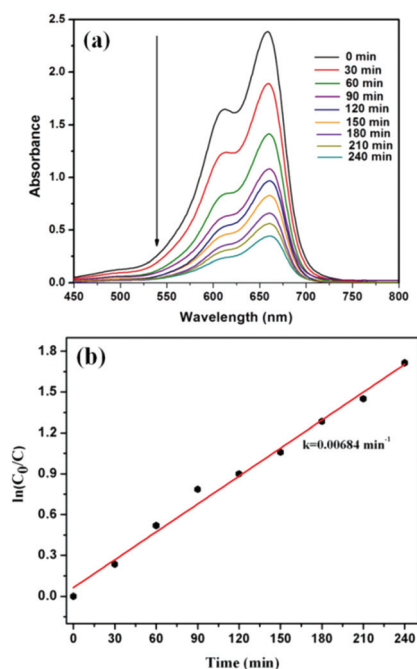
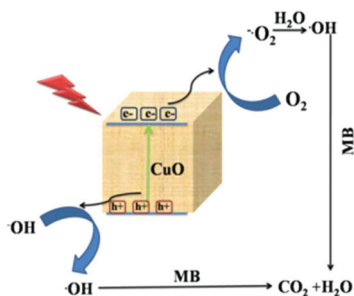
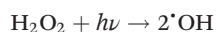
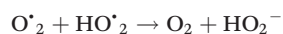
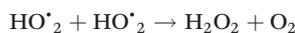
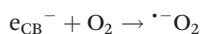


Fig. 8 (a) Absorption spectra of MB solution in the presence of CuO NCs upon visible light irradiation, (b) plot of $\ln(C_0/C)$ vs. irradiation time.



Scheme 4 CuO NC-catalysed visible light-induced degradation of MB.

superoxide radical $\cdot\text{O}_2^-$; it further reacts with H_2O to increase hydroxyl radical ($\cdot\text{OH}$) concentration, which is responsible for MB oxidation. The procedure is illustrated below.



The detailed mechanistic investigation on photo-catalytic bleaching of MB is available in literature.⁶⁹

In addition to direct CuO photo-excitation, dye degradation can also proceed *via* its sensitization of the semiconductor.⁷⁰ MB adsorbed at the surface of CuO NCs may undergo photo-excitation (absorption maximum, ~ 670 nm) and resultant electron injection into CuO CB, facilitating charge separation.

Experimental

Materials and methods

High-purity HEPES, salicylaldehyde, *N*-phenyl ethylenediamine, CuCl_2 and MnCl_2 are purchased from Sigma Aldrich (India). All reagents and solvents are of analytical reagent grade and used without further purification. Water with a resistivity of $18.2 \text{ M}\Omega \text{ cm}$ obtained from a Milli-Q, Millipore water purification system (Bedford, MA) is used in all experiments. A Shimadzu Multi Spec 2450 spectrophotometer is used for recording UV-vis spectra. FTIR spectra are recorded on a Shimadzu FTIR (model IR Prestige 21 CE) spectrophotometer. The steady state emission and excitation spectra are recorded with a Hitachi F-4500 spectro-fluorimeter. Systronics digital pH meter (model 335) is used for pH measurement. Single crystal X-ray diffraction data are collected on a Rigaku Ultra

X18 rotating anode diffractometer equipped with MAR345 image plate for **3** and on a Bruker SMART Apex II diffractometer equipped with a CCD area detector for **4** using $\text{Mo-K}\alpha$ (0.71073 \AA) radiation.

Size and morphology of CuO NCs are determined through Rietveld refinement of PXRD pattern and FESEM images. PXRD is recorded by Bruker D8 advanced diffractometer having Ni-filtered $\text{CuK}\alpha$ radiation within the range $2\theta = 20\text{--}80^\circ$.

Synthesis of 2-(((2(phenylamino)ethyl)imino)methyl)phenol (L)

L is synthesized by refluxing equimolar mixture of salicylaldehyde and *N*-phenyl ethylenediamine for 6 h in methanol.⁶³ The filtrate is kept at room temperature for slow evaporation. After a few days, yellow crystals of L are found. The yield is 86%. The purity of L is checked by ESI-MS (Fig. S17, ESI[†]) and ¹HNMR spectra (Fig. S18, ESI[†])

Synthesis of Cu(II) complex

Methanol solution of $\text{CuCl}_2 \cdot 6\text{H}_2\text{O}$ (85.24 mg; 0.5 mmol) is added slowly to the magnetically stirred solution of L (240 mg; 1 mmol) in dichloromethane at room temperature, and stirring is continued for 30 minutes. The solution is then filtered. Upon slow evaporation of the filtrate, green crystals suitable for single crystal X-ray diffraction are obtained. The yield is 80%. Significant crystal data and refinement parameters are given in ESI (Table S5, ESI[†]). FTIR (cm^{-1}) (Fig. S19; ESI[†]): $\nu(\text{N-H}, 2^\circ \text{ amine})$ 3342.64, $\nu(\text{CH}=\text{N})$ 1600.92, $\nu(\text{C-O phenyl})$ 1307.74; UV-Vis. (Fig. S20, ESI[†]): λ (nm) in ethanol-water (1/1, v/v), 361 nm, 269 nm and 232 nm.

The polymeric $[\text{L-Cu}^{2+}]$ complex is used as a precursor to prepare CuO NCs through calcination at 450°C for 5 h in air. The absorption and photoluminescence spectra of CuO NCs are presented in Fig. S21–22 (ESI[†]).

Synthesis of Mn(III) complex

Methanol solution of $\text{MnCl}_2 \cdot 4\text{H}_2\text{O}$ (95 mg; 0.5 mmol) is added slowly to a magnetically stirred solution of L (240 mg, 1 mmol) in dichloromethane at room temperature, and stirring is continued for 30 minutes. After filtration, the filtrate is kept for slow evaporation, and intense brown crystals suitable for X-ray diffraction are found after several days. Yield is 82%. Selected crystal parameters and refinement data are given in ESI (Table S5[†]).

FTIR (cm^{-1}) (Fig. S23; ESI[†]): $\nu(\text{N-H}, 2^\circ \text{ amine})$ 3331, $\nu(\text{CH}=\text{N})$ 1598.99, $\nu(\text{C-O phenyl})$, 1307.74. UV-Vis. (Fig. S24, ESI[†]): λ (nm) in ethanol-water (1/1, v/v) 382 nm, 330 nm, 242 nm and 222 nm.

Catalytic oxidation of 3,5-DTBC

To study the catecholase-like activity, $1 \times 10^{-4} \text{ mol dm}^{-3}$ solutions of **3** and **4** were treated with $1 \times 10^{-2} \text{ mol dm}^{-3}$ (100 equiv.) of 3,5-DTBC in methanol at room temperature under aerobic condition. For both **3** and **4**, absorbance of the quinone band increased significantly with time. The kinetics of the reaction was monitored by the initial rate method. The

concentration of the complex was fixed at 1×10^{-4} mol dm⁻³, whereas that of 3,5-DTBC was varied from 1×10^{-3} to 1×10^{-2} mol dm⁻³. Thus, 2 mL of 3,5-DTBC solution was quickly mixed with 0.04 mL of 5×10^{-3} mol dm⁻³ complex solution so that the final concentration of the complex in the mixture remained 1×10^{-4} mol dm⁻³. The rate constants vs. 3,5-DTBC concentration plot using Michaelis–Menten approach of enzymatic kinetics results in the Lineweaver–Burk (double reciprocal) plot. The rate constant (turn over number, K_{cat}), maximum velocity (V_{max}) and binding constant (K_{M}) are calculated from the plot of $1/V$ vs. $1/[S]$ using the equation $1/V = \{K_{\text{M}}/V_{\text{max}}\} \times \{1/[S]\} + 1/V_{\text{max}}$.

Photo-catalytic activity

Visible light-induced CuO NC-assisted photo-degradation of MB dye has been studied. CuO NCs (30 mg) are added to MB dye solution (1.2×10^{-4} M, 100 mL) and stirred in the dark for 30 min to establish the adsorption–desorption equilibrium of MB dye. After recording the absorbance at zero time, the solution is then irradiated with visible light. The absorbance of the solution is monitored at 30-minute intervals, and the percentage of dye degradation is calculated using the formula: degradation = $[(C_0 - C_t)/C_0] \times 100\%$, where C_0 and C_t are the absorbances of MB dye solution at zero and after “ t ” time, respectively.

Crystallography

Crystal data of **3** and **4** are summarized in Table S6 (ESI†). Data are corrected for Lorentz, polarization and absorption effects. The structures are solved by direct methods using SHELXS⁷¹ and refined by full-matrix least-squares with SHELXL⁷² and OLEX2 softwares.⁷³ Non-hydrogen atoms are refined with anisotropic thermal displacements. The hydrogen atoms are included in the structure refinement at the geometrically idealized positions with $U_{\text{iso}} = 1.2U_{\text{eq}}$ of the parent atoms. Molecular diagrams presented are drawn using the Mercury software.⁷⁴

Conclusion

In summary, we have designed and synthesized two polymeric complexes of Cu(II) and Mn(III). Their structures have been authenticated by single crystal X-ray diffraction analysis. An efficient catecholase activity is observed for both complexes. The Cu(II) complex specifically senses His with high selectivity and sensitivity under physiological conditions. We have developed a simple and efficient protocol for *N*-arylation of benzamide using several aryl iodides to prepare corresponding *N*-arylbzamidates in excellent yields using the Cu(II) complex as the catalyst. We have also described a facile thermal method of CuO NC synthesis using the Cu(II) complex as a precursor. Most importantly, CuO NCs exhibit visible light-induced excellent photo-catalytic activity to decolorize and degrade MB in aqueous suspension.

Conflicts of interest

There are no conflicts to declare.

Acknowledgements

B. Kumari gratefully acknowledges BU for fellowship. S. Kundu is thankful to DST for INSPIRE fellowship. K. Ghosh acknowledges SERB-DST NPDF (PDF/2016/000160) for financial assistance. The crystallographic studies were supported by CICECO-Aveiro Institute of Materials (UID/CTM/50011/2013), financed by National Funds through the FCT/MEC and co-financed by QREN-FEDER through COMPETE under the PT2020 partnership agreement.

Notes and references

- R. D. Archer and B. Wang, *Inorg. Chem.*, 1990, **29**, 39–43.
- I. Bertini, H. B. Gray, S. J. Lippard and J. S. Valentine, *Bioinorganic Chemistry*, University Science Books, Mills Valley, CA, USA, 1994.
- S. C. Bhatia, J. M. Bindlish, A. R. Saini and P. C. Jain, *J. Chem. Soc., Dalton Trans.*, 1981, 1773–1778.
- S. Chang, L. Jones, C. M. Wang, L. M. Henling and R. H. Grubbs, *Organometallics*, 1998, **17**, 3460–3465.
- K. K. Chaturvedi, *J. Inorg. Nucl. Chem.*, 1977, **39**, 901–905.
- J. Costamagna, J. Vargas, R. Latorre, A. Alvarado and G. Mena, *Coord. Chem. Rev.*, 1992, **119**, 67–88.
- D. Dey, G. Kaur, M. Patra, A. R. Choudhury, N. Kole and B. Biswas, *Inorg. Chim. Acta*, 2014, **421**, 335–341.
- F. Lebon, N. Boggetto and M. Ledecq, *Biochem. Pharmacol.*, 2002, **63**, 1863–1873.
- J. R. Prohaska, *Physiol. Rev.*, 1987, **67**, 858–901.
- C. L. Keen, Manganese, in *Biochemical of the Essential Ultratrace Elements* ed. E. Frieden, Plenum Press, New York, 1984, pp. 89–132.
- G. C. Cotzias, *Physiol. Rev.*, 1958, **38**, 503–532.
- K. Sumino, K. Hayakawa, T. Shibata and S. Kitamura, *Arch. Environ. Health*, 1975, **30**, 487–494.
- (a) T. E. Creighton, *Encyclopedia of Molecular Biology*, 1999, vol. 2, p. 1147; (b) G. N. Chen, X. P. Wu, J. P. Duan and H. Q. Chen, *Talanta*, 1999, **49**, 319–330.
- S. Zhang, C. Yang, W. Zhu, B. Zeng, Y. Yang, Y. Xu and X. Qian, *Org. Biomol. Chem.*, 2012, **10**, 1653–1658.
- (a) A. L. Jones, M. D. Hulett and C. R. Parish, *Immunol. Cell Biol.*, 2005, **83**, 106–118; (b) D. J. Sullivan Jr., I. Y. Gluzman and D. E. Goldberg, *Science*, 1996, **271**, 219–222; (c) F. W. G. Leebeek, C. Kluft, E. A. R. Knot and M. P. M. De Maat, *J. Lab. Clin. Med.*, 1989, **113**, 493–497; (d) H. Saito, L. T. Goodnough, J. M. Boyle and N. Heimbürger, *Am. J. Med.*, 1982, **73**, 179–182.
- M. Watanabe, M. E. Suliman, A. R. Qureshi, E. Garcia-Lopez, P. Bárány, O. Heimbürger, P. Stenvinkel and B. Lindholm, *Am. J. Clin. Nutr.*, 2008, **87**, 1860–1866.

- 17 Yu He, X. Wang, J. Zhu, S. Zhonga and G. Song, *Analyst*, 2012, **137**, 4005–4009.
- 18 Q. H. You, A. W. M. Lee, W. H. Chan, X. M. Zhua and K. C. F. Leung, *Chem. Commun.*, 2014, **50**, 6207–6210.
- 19 N. Tateda, K. Matsuhisa, K. Hasebe and T. Miura, *Anal. Sci.*, 2001, **17**, 775–778.
- 20 S. Wadud, M. M. Or-Rashid and R. Onodera, *J. Chromatogr. B: Anal. Technol. Biomed. Life Sci.*, 2002, **767**, 369–374.
- 21 L. Zhou, N. Yan, H. G. Zhang, X. M. Zhou, Q. S. Pu and Z. I. Hu, *Talanta*, 2010, **82**, 72–77.
- 22 J. Meng, W. Zhang, C. X. Cao, L. Y. Fan, J. Wu and Q. L. Wang, *Analyst*, 2010, **135**, 1592–1599.
- 23 M. Shahlaei, M. B. Gholivand and A. Pourhossein, *Electroanalysis*, 2009, **21**, 2499–2502.
- 24 M. A. Hortal, L. Fabbrizzi, N. Marcotte, F. Stomeo and A. Taglietti, *J. Am. Chem. Soc.*, 2003, **125**, 20–21.
- 25 Y. Zhang, C. M. Yang, W. P. Zhu, B. B. Zeng, Y. J. Yang, Y. F. Xu and X. H. Qian, *Org. Biomol. Chem.*, 2012, **10**, 1653–1658.
- 26 F. Pu, Z. Z. Huang, J. S. Ren and X. G. Qu, *Anal. Chem.*, 2010, **82**, 8211–8216.
- 27 P. Wu and X. P. Yan, *Biosens. Bioelectron.*, 2010, **15**, 485.
- 28 Z. Huang, J. Du, J. Zhang, X. Q. Yu and L. Pu, *Chem. Commun.*, 2012, **48**, 3412–3414.
- 29 L. Fabbrizzi, G. Francese, M. Licchelli, A. Perotti and A. Taglietti, *Chem. Commun.*, 1997, 581–582.
- 30 S. K. Sun, K. X. Tu and X. P. Yan, *Analyst*, 2012, **137**, 2124–2128.
- 31 L. Fabbrizzi, P. Pallavicini, L. Parodi, A. Perotti and A. Taglietti, *J. Chem. Soc., Chem. Commun.*, 1995, **23**, 2439–2440.
- 32 J. D. Swartz, C. P. Gulka, F. R. Haselton and D. W. Wright, *Langmuir*, 2011, **27**, 15330–15339.
- 33 (a) X. Qian, Y. Xiao, Y. Xu, X. Guo, J. Qian and W. Zhu, *Chem. Commun.*, 2010, **46**, 6418–6436; (b) A. P. de Silva, H. Q. NimalGunaratne, T. Gunnlaugsson, A. J. M. Huxley, C. P. McCoy, J. T. Rademacher and T. E. Rice, *Chem. Rev.*, 1997, **97**, 1515–1566.
- 34 (a) F. Pu, Z. Z. Huang, J. S. Ren and X. G. Qu, *Anal. Chem.*, 2010, **82**, 8211–8216; (b) M. Kruppa, C. Mandl, S. Miltschitzky and B. König, *J. Am. Chem. Soc.*, 2005, **127**, 3362–3365; (c) D. L. Ma, W. L. Wong, F. Y. Chan, W. H. Chuang, P. K. So, T. S. Lai, Z. Y. Zhou, Y. C. Leung and K. Y. Wong, *Angew. Chem.*, 2008, **47**, 3735–3739; (d) M. A. Hortal, L. Fabbrizzi, N. Marcotte, F. Stomeo and A. Taglietti, *J. Am. Chem. Soc.*, 2003, **125**, 20–21.
- 35 J. Du, Z. Huang, X. Q. Yu and L. Pu, *Chem. Commun.*, 2013, **49**, 5399–5401.
- 36 G. Klein and J.-L. Reymond, *Angew. Chem.*, 2001, **113**, 1821.
- 37 M. Fontecave and J.-L. Pierre, *Coord. Chem. Rev.*, 1998, **170**, 125–140.
- 38 L. Que Jr. and W. B. Tolman, *Nature*, 2008, **455**, 333–340.
- 39 J. Suh, *Acc. Chem. Res.*, 1992, **25**, 273–279.
- 40 P. Chaudhuri, M. Hess, U. Flörke and K. Wieghardt, *Angew. Chem.*, 1998, **37**, 2217–2221.
- 41 J. Reim and B. Krebs, *J. Chem. Soc., Dalton Trans.*, 1997, 3793.
- 42 S. Torelli, C. Belle, I. Gautier-Luneau, J. L. Pierre, E. Saint-Aman, J. M. Latour, L. Le Pape and D. Luneau, *Inorg. Chem.*, 2000, **39**, 3526–3536.
- 43 A. Neves, L. M. Rossi, A. J. Bortoluzzi, B. Szpoganicz, C. Wieszicki and E. Schwingel, *Inorg. Chem.*, 2002, **41**, 1788–1794.
- 44 J. Mukherjee and R. Mukherjee, *Inorg. Chim. Acta*, 2002, **337**, 429–438.
- 45 (a) P. Seth, M. G. B. Drew and A. Ghosh, *J. Mol. Catal. A: Chem.*, 2012, **365**, 154; (b) K. S. Banu, T. Chattopadhyay, A. Banerjee, M. Mukherjee, S. Bhattacharya, G. K. Patra, E. Zangrando and D. Das, *Dalton Trans.*, 2009, 8755–8764.
- 46 (a) S. Mukherjee, T. Weyhermüller, E. Bothe, K. Wieghardt and P. Chaudhuri, *Dalton Trans.*, 2004, 3842–3853; (b) S. Mukherjee, E. Rentschler, T. Weyhermüller, K. Wieghardt and P. Chaudhuri, *Chem. Commun.*, 2003, 1828–1829.
- 47 A. Guha, K. S. Banu, A. Banerjee, T. Ghosh, S. Bhattacharya, E. Zangrando and D. Das, *J. Mol. Catal. A: Chem.*, 2011, **338**, 51–57.
- 48 P. Chakraborty, S. Majumder, A. Jana and S. Mohanta, *Inorg. Chim. Acta*, 2014, **410**, 65–75.
- 49 S. Adhikari, S. Lohar, B. Kumari, A. Banerjee, R. Bandopadhyay, J. S. Matalobosc and D. Das, *New J. Chem.*, 2016, **40**, 10094–10099.
- 50 K. Moore and G. S. Vigee, *Inorg. Chim. Acta*, 1984, **91**, 53–58.
- 51 M. Malachowski, M. G. Davidson and J. N. Hoffman, *Inorg. Chim. Acta*, 1989, **157**, 91–94.
- 52 P. Sharma and G. S. Vigee, *Inorg. Chim. Acta*, 1984, 139.
- 53 M. A. Cabras and M. A. Zoroddu, *Inorg. Chim. Acta*, 1987, **135**, L19.
- 54 M. R. Malachowski and M. G. Davidson, *Inorg. Chim. Acta*, 1989, **162**, 199–204.
- 55 B. Srinivas, N. Arulsamy and P. S. Zacharias, *Polyhedron*, 1991, **10**, 731–736.
- 56 (a) M. Halder, Md. M. Islam, Z. Ansari, S. Ahammed, K. Sen and Sk. M. Islam, *ACS Sustainable Chem. Eng.*, 2017, **5**(1), 648–657; (b) H. Xu and C. Wolf, *Chem. Commun.*, 2009, 1715–1717.
- 57 (a) J. Yin and S. L. Buchwald, *Org. Lett.*, 2000, **2**, 1101–1104; (b) N. R. Deprez, D. Kalyani, A. Krause and M. S. Sanford, *J. Am. Chem. Soc.*, 2006, **128**, 4972–4973.
- 58 (a) J. C. Antilla, A. Klapars and S. L. Buchwald, *J. Am. Chem. Soc.*, 2002, **124**, 11684–11688; (b) M. M. Islam, M. Halder, A. S. Roy, S. Chatterjee, A. Bhaumik and S. M. Islam, *RSC Adv.*, 2016, **6**, 109692–109701; (c) Z. J. Quan, H. D. Xia, Z. Zhang, Y. X. Da and X. C. Wang, *Tetrahedron*, 2013, **69**, 8368–8374.
- 59 P. V. Kamat, *Chem. Rev.*, 1993, **93**, 267–300.
- 60 (a) T. Jiang, Y. Wang, D. Meng and M. Yu, *Superlattices Microstruct.*, 2015, **85**, 1–6; (b) M. Vaseem, A. Umar, Y. B. Hahn, D. H. Kim, K. S. Lee, J. S. Jang and J. S. Lee, *Catal. Commun.*, 2008, **10**, 11–16; (c) K. Mageshwari,

- R. Sathyamoorthy and J. Park, *Powder Technol.*, 2015, **275**, 150–156; (d) S. Kumar, C. M. A. Parlett, M. A. Parlett, M. A. Isaacs, D. V. Jowett, R. E. Douthwaite, M. C. R. Cockett and A. F. Lee, *Appl. Catal., B*, 2016, **189**, 226–232.
- 61 M. A. Hisham, M. E. Moustafa, Y. N. Moustafa and A. A. Ehab, *J. Mol. Struct.*, 2015, **1086**, 223–231.
- 62 A. Tadjarodi, O. Akhavan and K. Bijanzad, *Trans. Nonferrous Met. Soc. China*, 2015, **25**, 3634–3642.
- 63 A. Ghosh and D. Das, *Dalton Trans.*, 2015, **44**, 11797–11804.
- 64 A. W. Addison, T. N. Rao, J. Reedijk, J. van Rijn and G. C. Verschoor, *Dalton Trans.*, 1984, 1349–1135.
- 65 Z.-L. You, M. Zhang, D.-M. Xian, H.-H. Li and Q.-F. Weng, *Transition Met. Chem.*, 2012, **37**, 279–283.
- 66 (a) M. A. Hortalá, L. Fabbri, N. Marcotte, F. Stomeo and A. Taglietti, *J. Am. Chem. Soc.*, 2003, **125**, 20–21; (b) Y.-Y. Fu, H.-X. Li and W.-P. Hu, *Sens. Actuators, B*, 2008, **131**, 167–173; (c) Z. Huang, J. Du, J. Zhang, X. Q. Yu and L. Pu, *Chem. Commun.*, 2012, **48**, 3412–3414.
- 67 J. T. Hou, K. Li, K. K. Yu, M. Y. Wu and X. Q. Yu, *Org. Biomol. Chem.*, 2013, **11**, 717–720.
- 68 (a) S. Kundu, S. Sain, M. Yoshio, T. Kar, N. Gunawardhana and S. K. Pradhan, *Appl. Surf. Sci.*, 2015, **329**, 206–211; (b) L. Lutterotti, Maud Version 2.33, <http://www.ing.unitn.it/~maud/>.
- 69 A. Chithambararaj, N. S. Sanjini, A. C. Bose and S. Velmathi, *Catal. Sci. Technol.*, 2013, **3**, 1405–1414.
- 70 S. Tonda, S. Kumar, S. Kandula and V. Shanker, *J. Mater. Chem. A*, 2014, **2**, 6772–6780.
- 71 G. M. Sheldrick, *Acta Crystallogr., Sect. A: Found. Crystallogr.*, 2008, **64**, 112–122.
- 72 G. M. Sheldrick, *Acta Crystallogr., Sect. C: Struct. Chem.*, 2015, **71**, 3–8.
- 73 O. V. Dolomanov, L. J. Bourhis, R. J. Gildea, J. A. K. Howard and H. Puschmann, *J. Appl. Crystallogr.*, 2009, **42**, 339–341.
- 74 C. F. Macrae, I. J. Bruno, J. A. Chisholm, P. R. Edgington, P. McCabe, E. Pidcock, L. Rodriguez-Monge, R. Taylor, J. van de Streek and P. A. Wood, *J. Appl. Crystallogr.*, 2008, **41**, 466–470.